African Journal of Marine Science 2025, 47(4): 447–459
Printed in South Africa — All rights reserved

AFRICAN JOURNAL OF MARINE SCIENCE
ISSN 1814-232X EISSN 1814-2338
https://doi.org/10.2989/1814232X.2025.2554841

Influence of the Benguela Upwelling System on the genetic connectivity of blacktail seabream *Diplodus capensis* across southern Africa

WF Olivier[1], WM Potts[2], A-R Childs[2], C Santos[3], PW Shaw[4] and R Henriques[1]*

[1] Marine Genomics Group, Department of Biochemistry, Genetics and Microbiology, University of Pretoria, Pretoria, South Africa
[2] Department of Ichthyology and Fisheries Sciences, Rhodes University, Makhanda, South Africa
[3] Biology Department, Agostinho Neto University, Luanda, Angola
[4] Department of Life Sciences, Aberystwyth University, Aberystwyth, Wales, United Kingdom
** Corresponding author, e-mail: romina.henriques@up.ac.za*

Oceanographic features such as upwelling cells and currents contribute to shaping the evolutionary history of marine fishes, including species that may be important socio-economic resources. However, the impacts of these barriers are often cryptic and may change, particularly in a rapidly changing climate. Hence, sustainable fisheries management strategies need to take into consideration the influence of oceanographic barriers to the genetic structure of populations. Here, we evaluated the influence of the Benguela Upwelling System, a known barrier for warm-temperate fishes, on the evolutionary history of the blacktail seabream *Diplodus capensis* (family Sparidae), using eight microsatellite loci in conjunction with DNA barcoding of the cytochrome *c* oxidase 1 gene. *Diplodus capensis* is an important recreational and small-scale fishery species, distributed across southern Africa. Overall, there was significant genetic differentiation across the region, but the level of divergence varied with the genetic marker. Our results identified two isolated populations—in the northern and southern subsystems of the Benguela Upwelling System—with limited contemporary gene flow, and no sub-structuring detected within the subsystems. Because the species is vulnerable to exploitation, with declines in South Africa, our results suggest that management policies should aim at regional levels for the northern population (off Angola and Namibia), whereas the southern population (off South Africa) was identified as an isolated and highly connected population.

Keywords: adaptive capacity, fisheries management, gene flow, marine fish, microsatellites, mtDNA, phylogeography, Sparidae

Online supplementary material: The Supplementary Information, available at https://doi.org/10.2989/1814232X.2025.2554841, includes the microsatellite loci used for screening with their optimised amplification conditions (Table S1), the Bayesian clustering analyses and STRUCTURE admixture plots for K2 clusters using the relatedness pruned dataset (Figure S1), and the microsatellite genotypic data for all individuals (Table S2)

Introduction

In marine systems, multiple phylogeographic studies have identified common large-scale oceanographic barriers that can lead to the divergence of the populations or species on either side (Lett et al. 2024). One such barrier is the Benguela Upwelling System (BUS) off southwestern Africa, from southern Angola to South Africa. The BUS has unique characteristics, as it is bounded by two tropical currents, the Angola Current to the north, and the Agulhas current to the southeast, leading to the establishment of a warm-temperate transition zone. In addition, a perennial upwelling cell off central Namibia effectively divides the system into two subsystems: the northern and southern BUS (Hutchings et al. 2009). Previous phylogeographic studies have shown that these oceanographic features correlate well with genetic sub-structuring in coastal warm-temperate fishes, ranging from a shallow population structure that is not very genetically distinct, as seen in cold-tolerant species like the silver kob *Argyrosomus inodorus* (Henriques et al. 2015), to speciation events as seen for geelbeck croaker *Atractoscion aequidens* (Henriques et al. 2016a); in contrast, no significant genetic differentiation was found for the deep-water hake *Merluccius paradoxus*, indicating high gene flow across the BUS (Forde et al. 2025). Other studies have shown population structuring with gene flow across the BUS, as seen in the Cape horse mackerel *Trachurus capensis*, with shared mitochondrial DNA (mtDNA) haplotypes between Angola and South Africa (Healey et al. 2020); in the bluefish *Pomatomus saltatrix*, with evidence of secondary contact and unidirectional gene flow from the southern to the northern population (Reid et al. 2016); and in the shallow-water hake *M. capensis*, with seasonally dependent asymmetrical gene flow reported from the northern to the southern population (Kapula et al. 2022). Together, these findings suggest that the role of the BUS as an oceanographic barrier is multifactorial, and that it represents an important factor in understanding the evolutionary history of regional coastal marine fauna.

Although oceanographic barriers can strongly prevent gene flow (Lett et al. 2024), they are vulnerable to disruptions caused by climate change (Berger-Tal and Saltz 2019),

which can significantly impact their effectiveness as phylogeographic barriers (Pascual et al. 2017). For instance, a weakened barrier may allow secondary contact, where two previously isolated populations are back in contact (Reid et al. 2016). Additionally, two merged populations could be perceived as a single, more abundant, population because of increased catch rates, and thus misinterpreted as higher density leading to a heightened risk of overexploitation (Reiss et al. 2009). Climate change in the BUS has already led to the southward shift of a warm-temperate fish, the west coast dusky kob *Argyrosomus coronus*, from Angola into central Namibia (and possibly into South Africa), where it hybridises with *A. inodorus* (Potts et al. 2014; Pringle et al. 2023). Therefore, it is vital to understand and assess how regional oceanographic features impact the evolutionary history of warm-temperate species in the region, to inform sustainable management and conservation plans.

Members of the family Sparidae, including the blacktail seabream *Diplodus capensis*, are ecologically and economically important in southern Africa, supporting subsistence, recreational and small-scale fisheries (Comeros-Raynal et al. 2016). *Diplodus capensis* is found from Angola to southern Mozambique, but its abundance decreases from southern Namibia to the west coast of South Africa, likely because of colder sea surface temperatures and the species' preference for warmer waters (18.6–27 °C) (Yemane et al. 2004; Richardson et al. 2011a; Attwood et al. 2016). Biological studies also revealed significant differences between *D. capensis* from the northern and the southern BUS (Richardson et al. 2011a), as also observed for the zebra *D. hottentotus*, which exhibited genetic and morphological divergence across the region (Gwilliam et al. 2018). The BUS may thus act as a thermal barrier for *D. capensis* dispersal.

In addition, *D. capensis* is vulnerable to overexploitation because of its slow growth, long lifespan (Mann and Buxton 1998), sequential hermaphroditism (partial protandry) and strong site fidelity (Richardson et al. 2011a). In particular, partial hermaphroditism may make larger females more susceptible to fishing pressures, leading to skewed sex ratios and reduced fecundity. This, combined with strong site fidelity, which makes them particularly easy to target, further intensify the effects of exploitation. As a result, the South African population is considered depleted (DFFE 2023), despite its Least Concern status on the IUCN Red List of Threatened Species (Mann et al. 2009).

Therefore, the combination of biology, life history and oceanographic features suggest that *D. capensis* may be composed by isolated populations across the BUS. To test this hypothesis, we employed neutral molecular markers (microsatellites and mtDNA) to assess connectivity patterns, and understand if regional oceanographic features, namely the upwelling cell off central Namibia and the lower sea surface temperatures off the west coast of South Africa, impacted the evolutionary history of the species.

Materials and methods

Sampling and laboratory analyses

A total of 424 samples were collected from Angola, northern Namibia and South Africa between 2008 and 2011 (Figure 1). A fin clip was obtained from fish collected in markets, and subsistence/recreational fishers, and preserved in 96% ethanol. At the time of collection, no ethical clearance was required, as samples were obtained from fisheries. Total DNA was extracted using a phenol/chloroform-isoamyl alcohol method (Sambrook et al. 1989), and visualised in 2% agarose gel stained with ethidium bromide. All molecular data was generated between 2009 and 2011.

Eight cross-species microsatellites were selected for this study: DSMa16, DSMa27, DSMa34, DSMa48 (developed for *D. sargus*: Pérez et al. 2008), and Dvul4, Dvul33, Dvul61 and Dvul84 (developed for *D. vulgaris*: Roques et al. 2007). Amplification followed the original protocols, except for annealing temperatures and number of cycles (Supplementary Table S1). Forward primers were fluorescently labelled, and PCR products from multiple loci were combined in a multiplex mix based on colour and product size (Supplementary Table S1). Multiplexes were denatured in 10 µl of Hi-Di formamide (ABI) containing 0.2 µl of 600-LIZ® size standard per sample, for 5 min at 95 °C, and genotyped on an AB3500 Genetic Analyzer (Applied Biosystems). Genotype scores were generated using GENEMAPPER (ABIPrism).

A fragment of the mtDNA cytochrome oxidase 1 (mtDNA CO1) was amplified for a total of 165 individuals using FISHF1 and FISHR2 primers (Ward et al. 2005). PCR conditions followed the ones described by the authors, except for annealing temperature (48 °C). Obtained PCR products were cleaned using an enzymatic digestion: 0.45 U of Exonuclease I (Fermentas) and 0.9 U of Shrimp Alkaline Phosphatase (New England Biolabs) in 1× supplied buffer for 20 µl of PCR product. Digestions were incubated at 37 °C for 30 min, followed by 15 min at 80 °C, and 12 °C for 5 min. Cleaned products were sequenced in the forward and reverse directions, in an automated ABI-PRISM sequencer (Macrogen®), with the same primers used in the amplification. Raw sequences were trimmed and aligned using CLUSTAL-W in BIOEDIT.

Microsatellite data analyses

Microsatellite data were quality screened using Micro-Checker software (van Oosterhout et al. 2004) to assess stuttering and large allelic dropout, and the software program FreeNA (Chapuis and Estoup 2007) was used to detect the presence of null alleles. The statistical power of the dataset to detect subtle levels of population sub-structuring was tested in POWSIM (Ryman and Palm 2006), using a Monte Carlo Markov chain approach, by simulating divergence across eight populations, with an effective population size of 500, which drifted for 10 generations. Deviations to Hardy–Weinberg (HWE) and linkage equilibria were assessed in GenePop (Rousset 2008), using standard parameters. Statistical significance was assessed after Bonferroni correction for multiple tests (Bonferroni 1936). Relatedness levels between individuals were calculated using the Lynchrd estimator in the R package 'related' (Pew et al. 2015), as this estimator had a narrower 95% confidence interval (95% CI) estimate making it the better fit for the dataset. Relatedness was assessed over the entire dataset, as

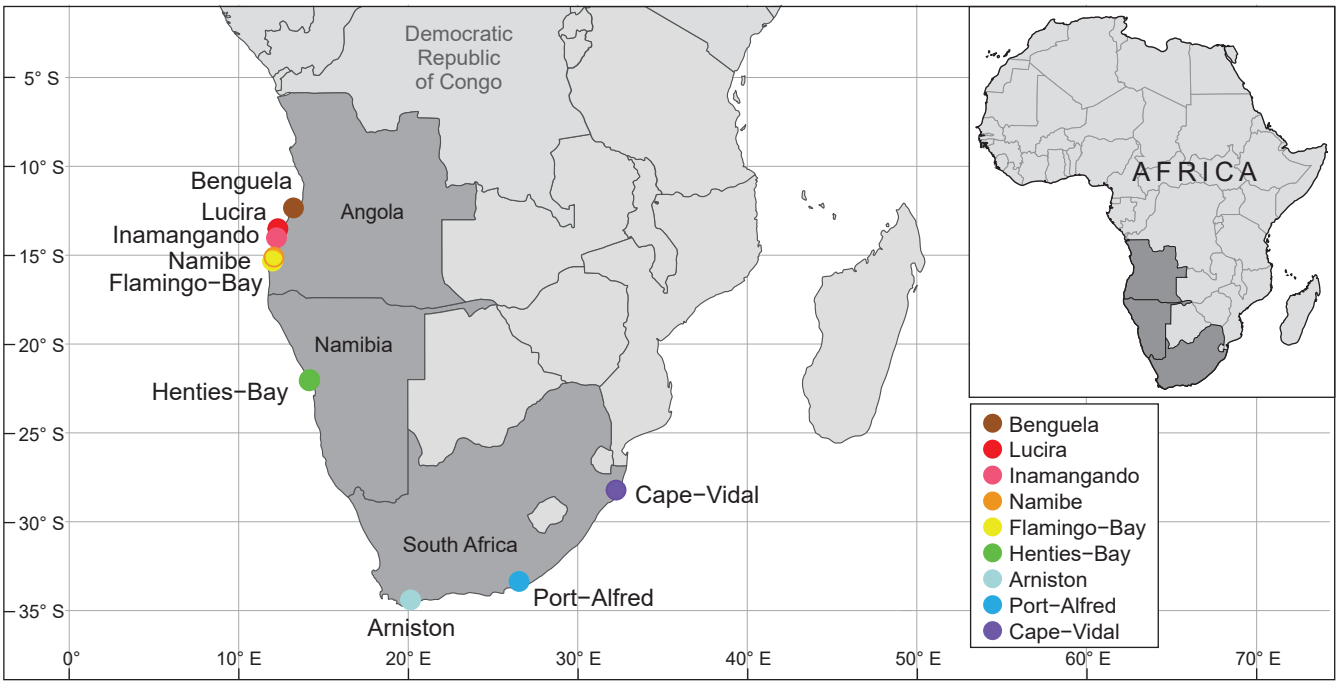

Figure 1: Sampling map for blacktail seabream *Diplodus capensis* in the Benguela Upwelling System, southeastern Atlantic

well as for the southern and northern regions separately. Relatedness levels were defined as: monozygotic twins (r = 1), full-siblings/parent-offspring (first-degree) (r = 0.5), half-siblings/grandparents (second-degree) (r = 0.25), first cousins (third-degree) (r = 0.125) or unrelated (r = 0) (Lynch and Ritland 1999). To filter for family structure, and owing to a wide 95% CI and limited sample size for some locations, individuals with a relatedness estimate of $r \geq 0.25$ were pruned from the dataset for additional Bayesian clustering analyses to confirm that patterns remained consistent if related individuals were removed.

Genetic diversity and population differentiation were estimated at different hierarchical levels: species, ocean, country and sampling location. Genetic diversity was calculated as observed and expected heterozygosity (H_O and H_E), allelic richness (AR), and inbreeding coefficients (F_{IS}) in the R package 'hierfstat' (Goudet 2005), per locus and over all loci, following Nei (1987), for the complete dataset. Statistical two-tailed t-tests were conducted in R to determine if there were significant differences across sampling sites.

Estimates of population differentiation were performed using complementary approaches. First, a principal component analysis (PCA) was used to visualise similarities between individuals, using the R package 'ade4' (Chessel et al. 1995). Second, Arlequin 3.5.2.2 (Excoffier and Lischer 2010) was used to calculate Weir and Cockerham (1984) pairwise F_{ST}, and pairwise Jost's D was calculated using the Microsoft Excel add-in GENALEX6.5 (Peakall and Smouse 2006), with statistical significance assessed after 10 000 iterations in both instances. Third, the coalescence approach of STRUCTURE (Pritchard et al. 2000) was used to detect cryptic levels of differentiation with a correlated allele frequencies model, for five runs for K = 1–16, with burn-in of 100 000 steps followed by 500 000 MCMC steps. StructureSelector (Li and Liu 2018) was used to calculate the most likely K with Clumpak (Kopelman et al. 2015) to visualise it. A second clustering analysis was done for a reduced dataset without related individuals, for a burn-in length of 100 000 steps followed by 250 000 Markov chain Monte Carlo steps. Fourth, hierarchal locus-by-locus analysis of molecular variance (AMOVA) using R_{ST} was conducted to test three structuring hypotheses: (i) panmixia; (ii) inter-Benguela structure (Angola and Namibia vs South Africa); and (iii) inter-country structure (Angola vs Namibia vs South Africa). Fifth, migration analyses were conducted with (i) BayesAss (Wilson and Rannala 2003), using the maximum proposal step lengths, 20 000 000 iterations with a burn-in period of 5 000 000, and a sampling interval of 1 000, which were checked for convergence and visualised as a gene flow plot using 'circlize' (Gu et al. 2014) in R; and (ii) Geneclass2 (Piry et al. 2004) was used to detect first-generation migrants, using the approaches of Baudouin and Lebrun (2000) and Paetkau (2004), for 1 000 simulated individuals.

Mitochondrial DNA data analyses

Genetic diversity levels and differentiation of mtDNA data were analysed in Arlequin 3.5.2.2. Genetic diversity was estimated through haplotype diversity, nucleotide diversity, the Ewens–Watterson test, and Tajima's D and Fu's Fs neutrality tests at the species, ocean and location level. To broadly estimate changes in demographic history, mismatch distribution analyses were calculated for the northern and southern populations, using the sudden spatial model in Arlequin, with statistical significance assessed after 10 000 permutations. Differentiation was estimated through

pairwise F_{ST} and locus-by-locus AMOVAs for the same three different hierarchical levels tested for microsatellites, with distance calculated based on the Tamura and Nei model (1993). Assessment of phylogeographic relationships was conducted via the reconstruction of a haplotype median-joining network analysis in PopART (Leigh et al. 2015).

Results

Microsatellites

No evidence of stuttering or large allele dropout was observed, and although FreeNA identified the presence of null alleles across several loci in different sampling sites, the observed frequencies were all below 15%. POWSIM analyses revealed that the dataset could accurately detect population structure for F_{ST} as low as 0.01 in 100% of cases. After correcting for multiple tests, only locus DS48 in the Port Alfred sample was found to not be in HWE. Similarly, no statistically significant linkage disequilibrium was observed after correcting for multiple tests. Therefore, all loci were retained for further analysis. Genotypes are listed in Supplementary Table S2.

The Lynchrd relatedness estimator identified 1 400 related pairs: 76 first-degree relatives ($r \geq 0.5$), and 1 324 second-degree relatives ($0.25 \leq r < 0.5$). However, only 17 of the 76 pairs were significantly related, with only 1 pair identified across the BUS (sampling sites Flamingo, Angola, and Cape Vidal, South Africa: lowest 95% CI interval >0.25). When the dataset was analysed per region (northern versus southern), 867 and 49 overall related pairs ($r > 0.25$) were found, corresponding to 1.6% and 0.9% of all the comparisons, respectively. However, of the 867 pairs, only 11 were statistically significant, and of the 49 pairs, only three were statistically significant. To assess their influence in the clustering patterns retrieved, we purged 233 individuals and ran STRUCTURE on the filtered dataset.

Overall, genetic diversity levels were high (H_O = 0.807, H_E = 0.849, AR = 26.529), whereas inbreeding was relatively low but positive (F_{IS} = 0.049) (Table 1). The northern region had lower diversity levels (H_O = 0.815, H_E = 0.833, AR = 18.571, F_{IS} = 0.021), than the southern region (H_O = 0.782, H_E = 0.841, AR = 21.176, F_{IS} = 0.071) (Table 1). Nevertheless, these metrics were not significantly different across the BUS ($p \geq 0.05$). Interestingly, Namibia exhibited the lowest values of diversity of the three countries, whereas estimates within the country showed that the sites at the edges of the distribution (Benguela and Cape Vidal) had lower values of diversity when compared with sites located at the core (Table 1).

Estimates of population differentiation revealed an overall pattern: samples from the northern BUS (Angola and Namibia) clustered together and somewhat isolated from samples from the southern BUS (South Africa). The scaled PCA based on sampling sites indicated grouping of northern versus southern sampling sites (Figure 2a). Grouping by country showed Angola and Namibia together, while South Africa grouped separately, but with some overlap with the northern sites (Figure 2b). No differentiation was observed within Angola nor South Africa (Figure 2c,d). The results obtained for pairwise Jost's D and F_{ST} reflected a similar pattern, with statistically significant (after correction for multiple comparisons) differentiation only observed between fish in the northern and southern BUS (F_{ST} = 0.044–0.045, Jost's D = 0.233–0.287, $p < 0.001$). No significant differentiation was observed between Angolan and Namibian sites, nor among sites within countries (Tables 2 and 3). Pairwise F_{ST} differentiation values ranged from F_{ST} = 0 for comparisons within each country, to F_{ST} = 0.068 for comparisons between Benguela (the northern most site in Angola) and Cape Vidal (the eastern most site in South Africa) (Table 3). Values of Jost's D followed a similar pattern but were consistently higher (Table 3), as expected.

Bayesian clustering analyses indicated two or three distinct clusters as the most likely structure for the unfiltered dataset (Figure 3a), and K = 2 for the dataset filtered for family structure (Supplementary Figure S1). For K = 2, the admixture plot showed a northern population that included Angola and Namibia, and southern population exclusively in South Africa, with high levels of admixture (Figure 3b); K = 3 provided no more meaningful structure visualisation by introducing a third thoroughly admixed layer over both regions (Figure 3c). The dataset filtered for relatives indicated a similar structure, but with lower resolution (Supplementary Figure S1b).

The hierarchical AMOVA (Table 4) for the panmixia hypothesis showed low but statistically significant differentiation (F_{ST} = 0.014, $p < 0.01$), suggesting weak but detectable genetic structure. The inter-Benguela subsystem hypothesis indicated slightly higher and significant differentiation among sampling sites within the same subsystem (F_{SC} = 0.032, $p < 0.01$), and statistically significant structure between subsystems (F_{CT} = 0.031, $p < 0.01$). The inter-country hypothesis resulted in statistically significant values of F_{SC} (0.026, $p < 0.01$) and F_{CT} (0.025, $p < 0.01$), but a negligible value of F_{ST} (0.001, $p \geq 0.5$), indicating potential finer-scale structure between sampling sites within countries.

Migration analyses using BayesAss revealed very low levels of statistically significant migration rates across the BUS, with most migrants detected within each subsystem (Figure 4). The only migration rates that were statistically significant were the migration from Port Alfred to other southern sites, from Lucira to other northern sites, but also from Lucira to Port Alfred (m = 0.075) (Figure 4). GeneClass2 detected 9 individuals as statistically significant first-generation migrants across sites ($p < 0.01$). Overall, 1 southern first-generation migrant was detected in the northern region and 3 northern first-generation migrants were detected in the southern region, with at least 1 individual of significantly different assignment probabilities in either direction. Benguela had 1 migrant from Flamingo. Henties Bay had 2 first-generation migrants in total, from Lucira and Namibe. Flamingo had 1 migrant from Henties Bay, and Lucira had 1 migrant from Arniston. Port Alfred also had 2 first-generation migrants, 1 each from Namibe and Flamingo, and Cape Vidal had 1 first-generation migrant from Port Alfred and 1 from Benguela.

Mitochondrial DNA

After filtering, a fragment of 619 bp was obtained for mtDNA CO1 for 162 individuals, resulting in 24 haplotypes:

Table 1: Average genetic diversity estimates for *Diplodus capensis* in the Benguela Upwelling System (BUS) across all loci at different grouping levels, based on eight microsatellite loci. *n* = number of samples; AR = allelic richness; H_O = observed heterozygosity; H_E = expected heterozygosity; F_{IS} = inbreeding coefficient; LL = F_{IS} lower limit; UP = F_{IS} upper limit. An asterisk (*) marks statistically significant value of F_{IS}

			n	AR	H_O	H_E	F_{IS}	LL	UP
Per location	Angola	Benguela	81	10.051	0.804	0.830	0.032*	0.003	0.058
		Lucira	72	10.118	0.828	0.833	0.005	−0.042	0.048
		Namibe	69	10.125	0.820	0.834	0.016	−0.017	0.045
		Flamingo	78	10.349	0.806	0.836	0.034	−0.007	0.081
	Namibia	Henties Bay	21	9.732	0.831	0.823	−0.015	−0.084	0.051
	South Africa	Arniston	29	11.550	0.821	0.852	0.038	−0.004	0.078
		Port Alfred	60	11.010	0.773	0.840	0.080*	0.044	0.116
		Cape Vidal	14	11.125	0.741	0.821	0.107	−0.003	0.214
Per country	Angola		300	10.805	0.814	0.833	0.023	−0.002	0.051
	Namibia		21	10.395	0.831	0.823	−0.015	−0.079	0.054
	South Africa		103	12.104	0.782	0.841	0.071*	0.043	0.101
Per BUS region	Northern		321	18.571	0.815	0.833	0.021	−0.002	0.048
	Southern		103	21.176	0.782	0.841	0.071*	0.042	0.101
Species			424	26.529	0.807	0.849	0.049*	0.029	0.074

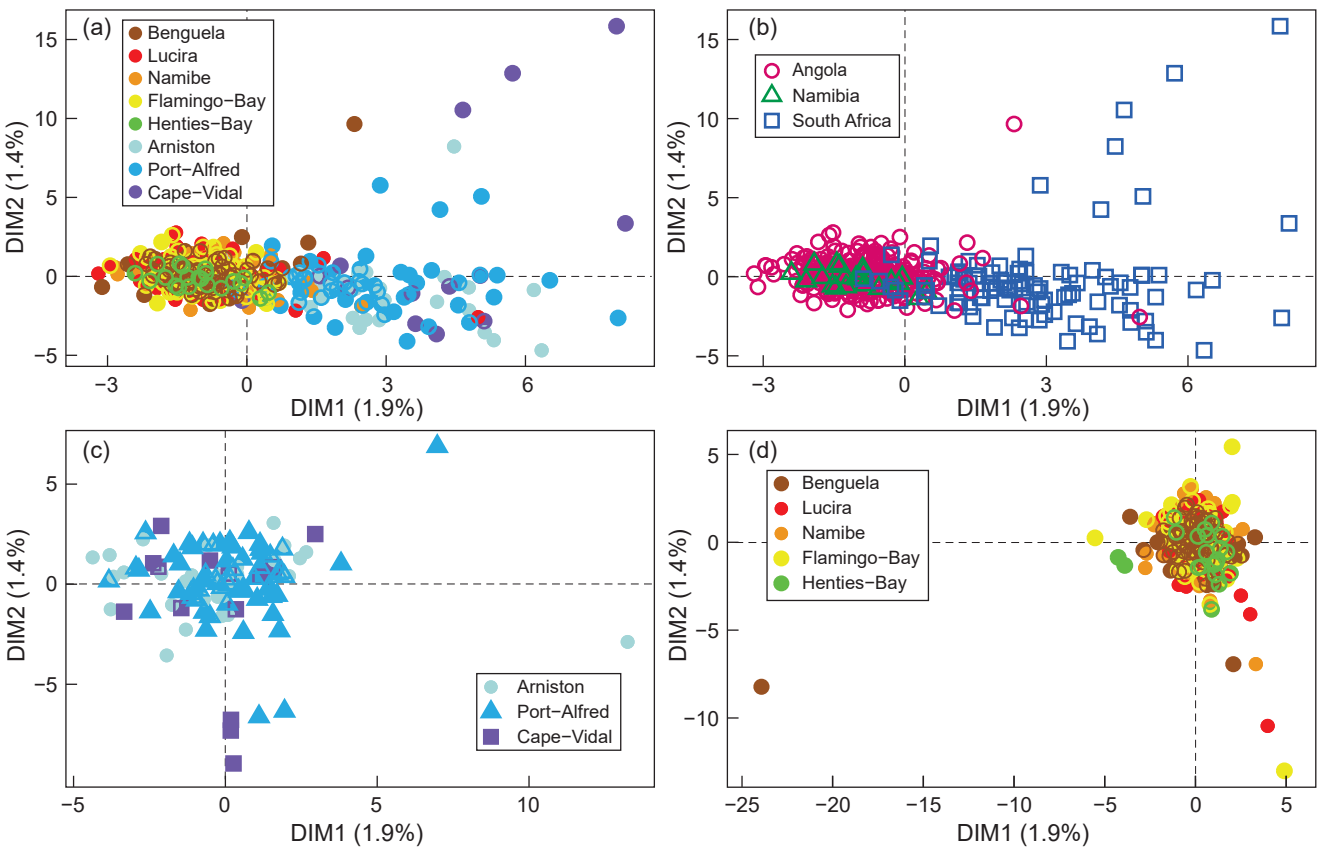

Figure 2: Scaled principal components analysis for *Diplodus capensis*, based on eight microsatellite markers for: (a) all sampling sites, (b) country, (c) southern sites, and (d) northern sites, including the percentage of variance (%) explained by each principal component (Dim1 and Dim2)

17 private, 5 shared by more than 2 individuals, and 2 commonly shared within the northern and southern BUS (GenBank accession nos. JX192287–JX192451) (Table 5; Figure 5). Overall, moderate haplotype diversity (*h* = 0.715) and relatively low nucleotide diversity (π = ~0.004) were observed for the species (Table 5). The Ewens–Waterson observed *F*-statistic (0.289) suggested that the slightly reduced population diversity did not significantly differ from neutral expectations (Ewens–Watterson probability of ~1), whereas Fu's *Fs* (−10.987)

and Tajima's *D* (−1.196) were all negative. The northern region had *h* = 0.546 and π = 0.001, while the southern region had *h* = 0.303 and π = 0.001. Haplotype diversity was highest in Benguela and Lucira (~0.670–0.700) and lowest in Arniston and Henties Bay (~0.105–0.279). Nucleotide diversity showed a similar pattern as haplotype diversity, with Benguela, Lucira and Flamingo showing higher diversity and Arniston the lowest (Table 5). The northern and southern regions both had negative neutrality estimates (south: *Fs* = −4.473, *D* = −1.875; north: *Fs* = −18.979, *D* = −1.993), with an Ewens–Watterson *F*-statistic range of 0.335 < *F* < 0.900 (Table 5).

Mismatch distribution analyses did not allow a rejection of the null hypothesis of geographical expansion, but estimates of time since expansion (in mutational units) were higher for the northern (τ = 0.782) than for the southern (τ = 0.400) population.

As seen for the microsatellite dataset, pairwise ϕ_{ST} values were significantly different from zero for northern versus southern comparison (ϕ_{ST} = 0.855, $p < 0.01$) (Table 6), as well as any comparisons involving northern versus southern sites (ϕ_{ST} = 0.833–0.953, $p < 0.001$) (Table 7). Differentiation was not significant between locations within each region, after correcting for multiple tests.

The hierarchical AMOVA (Table 4) testing for panmixia showed highly significant F_{ST} (0.752, $p < 0.01$), suggesting strong genetic differentiation among populations and rejection of panmixia. The inter-Benguela subsystem hypothesis test indicated very large and significant levels of genetic structure between Benguela subsystems (F_{CT} = 0.862, $p < 0.01$), with significant differentiation among all sampling sites (F_{ST} = 0.866, $p < 0.05$). The inter-country hypothesis testing indicated significant genetic differentiation between countries (F_{CT} = 0.822, $p < 0.01$).

The haplotype network analysis (Figure 5) indicated a clear separation between the northern and southern populations as the locations from the northern Benguela subsystem shared no haplotypes with the southern subsystem indicating complete lineage sorting.

Table 2: Genetic differentiation levels per country measured as the pairwise Weir and Cockerham (1984) F_{ST} estimator (below diagonal) and Jost's *D* (above diagonal), based on eight microsatellite markers for *Diplodus capensis*. **p* < 0.05; ***p* < 0.01; *p* < 0.00167 (with Bonferroni-corrected α in bold)

	Angola	Namibia	South Africa
Angola	–	−0.015	**0.233****
Namibia	0.001	–	**0.287****
South Africa	**0.044****	**0.045****	–

Discussion

Genetic diversity of D. capensis *across the BUS*

Estimates of genetic diversity for *D. capensis* based on microsatellite data revealed relatively high levels, with an overall H_O of 0.807 and values across sampling sites ranging $0.773 < H_O < 0.831$, despite the use of cross-specific markers. Although direct comparisons are not reliable across species and microsatellite loci, the values here reported are similar in range to those of other sparid species, such as the gilt-head seabream *Sparus aurata* in the Adriatic Sea (H_O = 0.72–0.83, H_E = 0.73–0.84) (Žužul et al. 2022), but higher than for the zebra *D. hottentotus* in the BUS (Gwilliam et al. 2018), despite the use of the same microsatellite markers as the present study (average across loci $0.292 < H_O < 0.385$). Inbreeding coefficients and allelic richness were lower in the northern region (F_{IS} = 0.021, AR = 18.571) than in the southern region (F_{IS} = 0.071, AR = 21.176). This pattern was consistent at country level and over all sampling sites. Nevertheless, observed heterozygosity was similar across Angola and Namibia (H_O ~ 0.82), and slightly higher than in South Africa (H_O = 0.782). A higher F_{IS} in the southern region may result from a heterozygote decrease as expected from a Wahlund effect—wherein different genetic units are sampled as a single population. In fact, dispersal patterns of *D. capensis* in South Africa revealed up to five potential subpopulations, linked to oceanographic features (Muller et al. 2024), and may thus point to subtle subpopulation differentiation within the southern population. However, other biological reasons could explain this difference in inbreeding coefficients. For example, chaotic genetic patchiness (CGP) (Johnson and Black 1992) owing to sweepstake recruitment events, temporal recruitment variability or even larval cohesion (where larvae remain together: McKeown et al. 2017), may explain the inflated F_{IS} of the southern population. In fact, CGP was identified as a possible explanation for fluctuations in diversity of *Merluccius paradoxus* across the BUS, because of years of poor recruitment (Henriques et al. 2016b). To identify the mechanism responsible for higher F_{IS} in the southern region, it would be necessary to increase the number of sampling locations across South Africa, and include a temporal component to evaluate how drift could impact estimates of diversity.

Table 3: Genetic differentiation levels based on pairwise F_{ST} (below diagonal) and pairwise Jost's *D* (above diagonal) per sampling region, based on eight microsatellite markers for *Diplodus capensis*. **p* < 0.05; ***p* < 0.01; *p* < 0.00167 (with Bonferroni-corrected α in bold)

	Benguela	Lucira	Namibe	Flamingo	Henties Bay	Arniston	Port Alfred	Cape Vidal
Benguela	–	0.006	0.000	0.000	0.029*	**0.248****	**0.236****	**0.342****
Lucira	0.001	–	0.008	0.002	0.012	**0.213****	**0.212****	**0.301****
Namibe	0.000	0.001	–	0.000	0.033*	**0.225****	**0.223****	**0.328****
Flamingo	0.000	0.000	0.000	–	0.020	**0.215****	**0.217****	**0.319****
Henties Bay	0.002	0.000	0.005	0.000	–	**0.248****	**0.249****	**0.320****
Arniston	0.045**	0.038**	0.042**	**0.039****	**0.043****	–	−0.006	−0.002
Port Alfred	**0.043****	**0.038****	**0.041****	**0.039****	**0.043****	0.000	–	0.012
Cape Vidal	0.068**	0.060**	0.067**	0.064**	0.065**	0.002	0.004	–

Genetic diversity estimates based on mtDNA data were relatively lower than the ones obtained for the nuclear DNA dataset, but consistently higher in Angola than in Namibia and South Africa. In addition, the observed estimates for Tajima's *D* and Fu's *Fs*, suggest an historical population contraction (bottleneck or founder effect) followed by a subsequent expansion (Tajima 1989; Fu 1997). These findings are further supported by the observed star-shaped

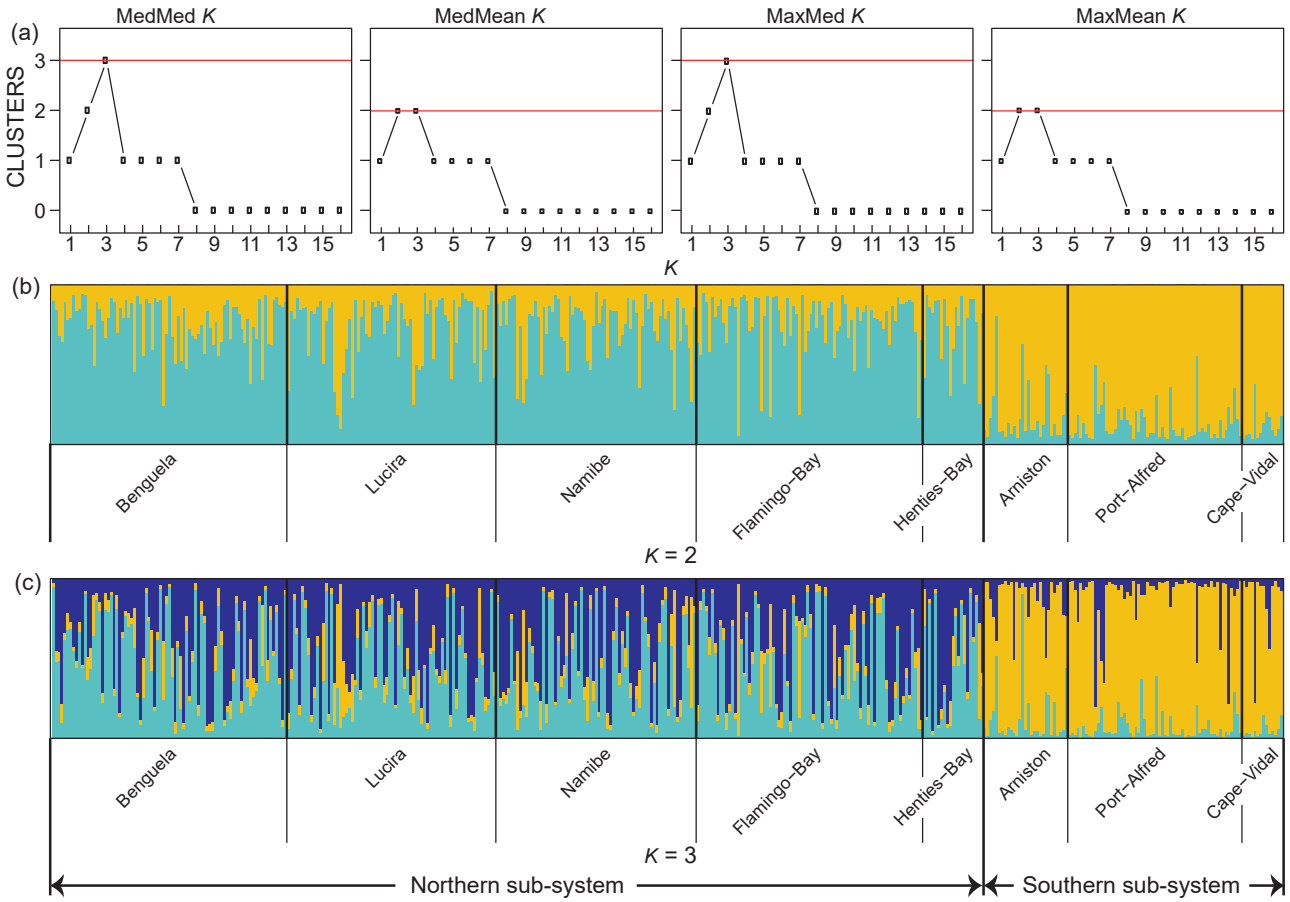

Figure 3: (a) Bayesian clustering analyses conducted for *Diplodus capensis*, based on eight microsatellite loci, including plots of MedMed *K*, MedMean *K*, MaxMed *K* and MaxMean *K* to estimate the likely *K*. (b, c) STRUCTURE admixture plots for K2 and K3 clusters, respectively, with sampling location depicted on the *x*-axis

Table 4: Hierarchal microsatellite locus-by-locus AMOVA testing of different hypotheses for the population structure of *Diplodus capensis* in the Benguela Upwelling System. *$p < 0.05$; **$p < 0.01$; $p < 0.00167$ (with Bonferroni-corrected α in bold)

Marker	Hypothesis tested	Source of variation	Variation	Fixation index	
Microsatellites	Single group structure model	Among sampling sites	1.431	F_{ST}	**0.014****
		Within sampling sites	98.569		
	Between country group structure model	Among groups	2.516	F_{CT}	**0.025****
		Among sampling sites within groups	0.122	F_{SC}	**0.026****
		Within sampling sites	97.362	F_{ST}	0.001
	Inter-Benguela subsystem group structure model	Among groups	3.133	F_{CT}	**0.031****
		Among sampling sites within groups	0.062	F_{SC}	**0.032****
		Within sampling sites	96.806	F_{ST}	0.001
mtDNA	Single group structure model	Among sampling sites	75.218	F_{ST}	**0.752****
		Within sampling sites	24.782		
	Between country level structure model	Among groups	82.218	F_{CT}	**0.822****
		Among sampling sites within groups	0.540	F_{SC}	**0.030****
		Within sampling sites	17.242	F_{ST}	0.828
	Inter-Benguela subsystem group structure model	Among groups	86.202	F_{CT}	**0.862****
		Among sampling sites within groups	0.367	F_{SC}	**0.027****
		Within sampling sites	13.431	F_{ST}	0.866*

Figure 4: Gene flow diagram based on BayesAss migration analyses results for *Diplodus capensis* based on eight microsatellite loci and across eight sampling sites: Benguela (BN), Lucira (LC), Namibe (NE), Flamingo Bay (FB), Henties Bay (HB), Arniston (AN), Port Alfred (PA), and Cape Vidal (CV). Colours represent the estimated site of origin; relative line thickness represents the estimated ratio of individuals

phylogeographic network, which was dominated by two main haplotypes, shared by the majority of individuals, from which private haplotypes—or haplotypes shared by a few individuals—differed by one to two mutational steps.

A possible reason for the higher nucleotide and haplotype diversities and lower inbreeding coefficient and allelic richness in the northern sites, may be a more recent (and/or severe) population contraction in the southern region. This pattern could be the result of a population history where two founder populations, on in the northern region and one in the southern region, underwent population expansions at different points in time. In fact, estimates of time since expansion (τ) based on the mismatch distribution analyses showed a higher value for the northern population (0.782) versus the southern population (0.400) based on the geographical expansion model. Given the known high uncertainty in estimating time since expansion based on mismatch distribution parameters (Grant 2015), we provide here a rough estimate for illustration purposes only, that should not be taken at face value. With this caveat, assuming a general mutation rate of 2% per million years per nucleotide for mtDNA CO1 and a sequence length

Table 5: Mitochondrial genetic diversity levels and neutrality tests for *Diplodus capensis* based on 619 bp of mtDNA CO1. *n* = number of individuals; *H* = number of haplotypes; *h* = haplotype diversity; π = nucleotide diversity; EWoF = Ewens–Waterson neutrality test observed *F*-statistic; EWeF = Ewens–Waterson neutrality test expected *F*-statistic; *Fs* = Fu's neutrality test; *D* = Tajima's neutrality test. **p* < 0.05; ***p* < 0.01; and *p* < 0.00556 for locations, *p* < 0.0167 for countries, and *p* < 0.025 for regions (with Bonferroni-corrected α in bold)

Sampling site	*n*	*H*	*h*	π	EWoF	EWeF	*Fs*	*D*
Benguela	20	8	0.700	0.002	0.335	0.210	**−5.149****	−1.665*
Lucira	20	6	0.674	0.002	0.360	0.296	−2.229*	−0.866
Inamangando	16	3	0.425	0.001	0.602	0.538	−0.290	−0.330
Namibe	20	4	0.490	0.001	0.535	0.443	−1.024	−1.260
Flamingo	19	7	0.667	0.002	0.368	0.241	**−3.876****	−1.050
Angola	95	18	0.596	0.001	0.411	0.142	−18.336**	−1.981**
Henties Bay, Namibia	20	3	0.279	0.000	0.735	0.553	−1.206*	−1.141
Northern population (Namibia and Angola)	115	18	0.546	0.001	0.458	0.150	**−18.980****	**−1.993****
Arniston	19	2	0.105	0.000	0.900	0.729	−0.838	−1.165
Port Alfred	12	3	0.318	0.001	0.536	0.429	−0.614	−1.629
Cape Vidal	17	4	0.493	0.001	0.708	0.513	−1.537*	−1.096*
Southern population (South Africa)	48	6	0.303	0.001	0.703	0.370	**−4.473****	**−1.875****
Species	163	24	0.715	0.004	0.289	0.119	**−10.987****	−1.196

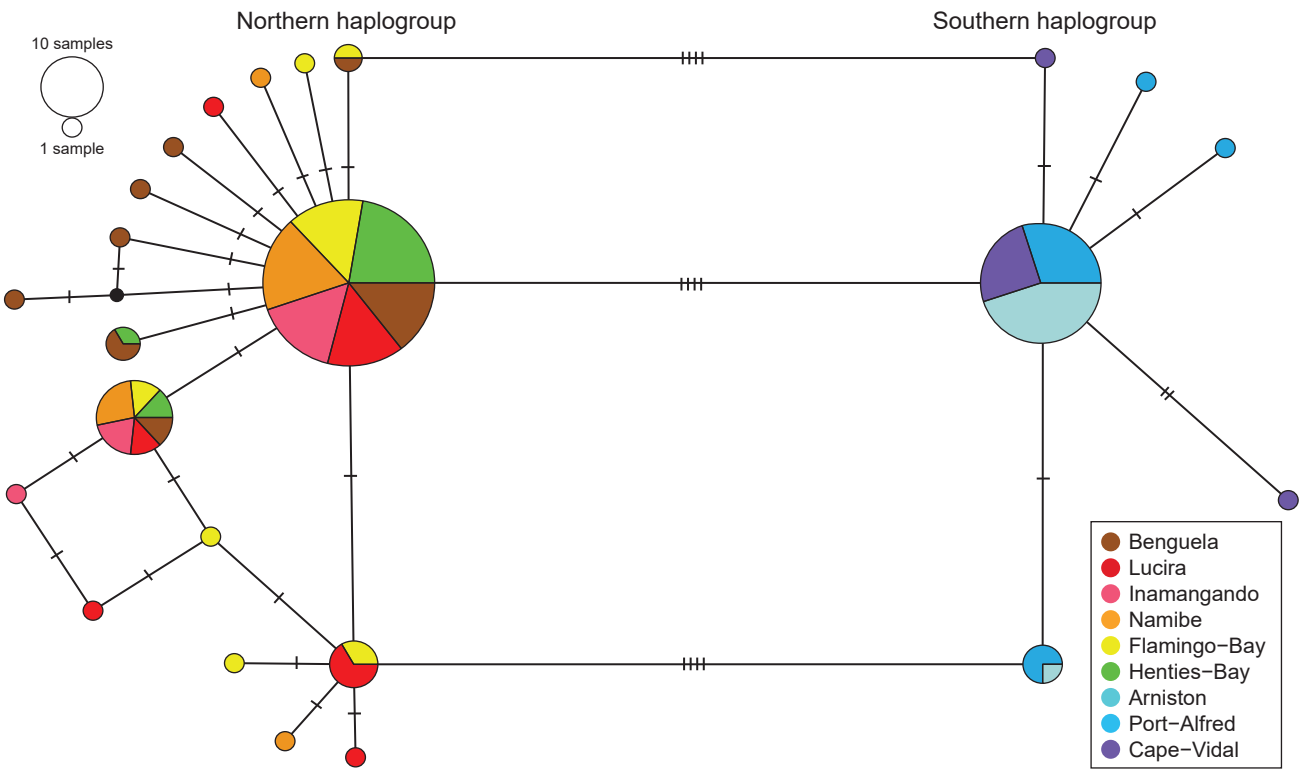

Figure 5: Median-joining haplotype network analysis using mtDNA CO1 sequences of *Diplodus capensis* across nine sampling sites, showing a northern and a southern haplogroup across the Benguela Upwelling System. Each node represents a unique haplotype; the size of the node represents its frequency, and each notch on connecting lines represents the number of nucleotide substitutions between haplotypes

of 619 bp, the northern population would have expanded roughly 29 500 years ago, whereas the southern population would have expanded more recently at ~16 150 years ago. In both cases, these estimates pre-date the end of the Last Glacial Maximum (12 000–10 000 years ago), which have also been reported for other marine fish across the BUS. For example, *Argyrosomus inodorus* showed higher haplotype and nucleotide diversity, as well as time since expansion, but also lower allelic richness and F_{IS} for the Namibian population compared with the South African population (Henriques et al. 2015), as well as compared with *Atractoscion aequidens* (Henriques et al. 2014). Similarly, *D. hottentotus* showed higher haplotype diversity in the northern population than in the southern population

(Gwilliam et al. 2018). If these times of expansion hold, it would suggest that the northern populations of warm-temperate coastal species in the BUS region have expanded earlier, probably from refugia, when compared with the southern populations. Additional reconstruction of demographic history through time would be required to assess the rates of recovery of these populations, and potentially identify historical refugia, common to warm-temperate species across the BUS region.

Patterns of population differentiation of D. capensis *across the BUS*

Evidence for cross-region gene flow?

Assessment of population structure indicated significant differentiation across the BUS with two distinct genetic clusters (northern and southern) retrieved, regardless of the method or marker used. Pairwise comparisons of genetic differentiation based on the microsatellite dataset revealed significant divergence between the northern (Angola and Namibia) and southern (South Africa) regions, with F_{ST} = 0.044 and Jost's D = 0.262. Pairwise differentiation using mtDNA was much higher (F_{ST} = 0.863), supporting the absence of shared haplotypes and complete lineage sorting seen in the phylogeographic network. Similar findings were reported for *D. hottentotus* across the same sampling region and using the same microsatellite markers; however, pairwise differentiation levels based on microsatellite data for this species were higher (F_{ST} = 0.23, p < 0.05) than reported here for *D. capensis*, whereas estimates based on mtDNA were lower (F_{ST} = 0.5, p < 0.05), as a shared haplotype was observed between Angola and South Africa, interpreted by the authors as retention of ancestral polymorphisms (Gwilliam et al. 2018).

The AMOVA results further supported a northern versus southern pattern of differentiation, regardless of the marker used. Similarly, clustering analyses based on microsatellite data retrieved two groups (northern versus southern) as the most likely population sub-structuring hypothesis for the dataset. These results are similar to those reported for other warm-temperate species in the region, with northern and southern groups described for *A. aequidens*, leerfish *Lichia amia* and *M. capensis*, while no differentiation was observed within groups (Henriques et al. 2012, 2016b). In particular, complete lineage sorting for the mtDNA was reported for the first two species, which have similar thermal requirements as *D. capensis*.

However, the AMOVA results also indicated significant fixation indexes among sampling sites within country and regional groups suggesting the presence of finer-scale sub-structuring within the two main populations, for both microsatellite and mtDNA data. This would align with the previous work of Muller et al. (2024) that identified up to five potential subpopulations associated with oceanographic conditions in South Africa. These findings, combined with estimates of dispersal patterns and the fixation indexes reported here, imply finer-scale structuring within the southern population for which neutral markers lack sufficient resolution to identify.

Despite the identification of distinct genetic clusters, clustering analyses using microsatellite data exhibited widespread admixture, with relatedness and migration analyses also suggesting very low ongoing connectivity across the BUS. In fact, relatedness analyses revealed one second-degree related pair between Flamingo and Cape Vidal (~4 000 km apart), while migration analyses suggested the presence of low levels of connectivity mostly from the northern to the southern subsystem, with first-generation migrants also identified. Similar connectivity findings were reported for *D.* sargus in the Mediterranean Sea, with a maximum distance of 2 221 km observed between one full-sibling pair, and additional five related pairs separated by >1 300 km (Manel et al. 2023). However, most of the literature on *D. capensis* do not support the likelihood of this migration pattern, owing to temperature requirements, dispersal abilities and larval duration. *D. capensis* relies primarily on larval dispersion (Cele et al. 2016), which could result in passive dispersal influenced by currents. The Benguela current, however, flows against the observed migration pattern from south

Table 6: Genetic differentiation levels measured as pairwise ϕ_{ST} values per country based on 619 bp of mtDNA CO1 for *Diplodus capensis*. *p < 0.05; **p < 0.01; p < 0.00167 (with Bonferroni-corrected α in bold)

	Angola	Namibia	South Africa
Angola	–		
Namibia	−0.002	–	
South Africa	**0.855****	**0.922****	–

Table 7: Genetic differentiation levels based on pairwise ϕ_{ST} (below diagonal) per sampling region, based on 619 bp of mtDNA CO1 for *Diplodus capensis*. *p < 0.05; **p < 0.01; p < 0.00167 (with Bonferroni-corrected α in bold)

	Benguela	Lucira	Inamangando	Namibe	Flamingo	Henties Bay	Arniston	Port Alfred	Cape Vidal
Benguela	–								
Lucira	0.073*	–							
Inamangando	0.013	0.070	–						
Namibe	0.006	0.042	−0.034	–					
Flamingo	0.029	0.000	0.028	0.001	–				
Henties Bay	0.000	0.097*	0.017	0.000	0.043	–			
Arniston	0.880**	0.878**	0.932**	**0.915****	**0.885****	**0.953****	–		
Port Alfred	**0.839****	**0.835****	**0.885****	**0.872****	**0.842****	**0.909****	0.015	–	
Cape Vidal	**0.834****	**0.833****	**0.888****	**0.873****	**0.839****	**0.917****	0.024	0.039	–

to north, and at a speed similar to that reported for the species' late-stage mean larval swimming abilities (17–23 cm s^{-1} versus 18 cm s^{-1}, respectively) (Shannon 1985; Wedepohl et al. 2000; Pattrick and Strydom 2009). This suggests that *D. capensis* would still likely need refuge along the BUS to facilitate migration, which would make migration in one generation unlikely.

Unlike *D. hottentotus* (Gwilliam et al. 2018), the mtDNA dataset exhibited reciprocal monophyly between *D. capensis* from the northern and southern subsystems, suggesting an historical divergence and the absence of ongoing gene flow. Disparity between marker types is mathematically expected if they experience differential effects from evolutionary forces such as drift, mutation, migration, selection, as well as homoplasy, effective population size or sex-biased dispersal (Buonaccorsi et al. 2001). As a result of maternal inheritance, the complete lineage sorting observed for *D. capensis* mtDNA would make female-biased migration and sex-independent larval dispersal unlikely as these would result in ongoing mtDNA gene flow. Our findings could thus suggest female philopatry and male-mediated dispersal, as seen in bonnethead *Sphyrna tiburo* (Portnoy et al. 2015). However, in *D. capensis*, male-biased dispersal could still be expected to result in ongoing mtDNA gene flow caused by their partial protandry (Richardson et al. 2011a), as some males could be expected to change to females after migration allowing individuals to add mtDNA to the gene pool of the receiving population.

It is likely that the hypothesis of no ongoing gene flow is indeed correct, and that the observed admixture based on microsatellite data is an artefact of incomplete lineage sorting and retention of ancestral polymorphisms owing to a relatively recent divergence time and the larger effective population size of the nuclear genome in comparison with mtDNA. Population differentiation in the absence of migration will result from genetic drift, which becomes inefficient in larger populations (Castro et al. 1998). Therefore, it would be seen earlier in mtDNA than in the nuclear genome.

However, if ongoing gene flow is truly possible for *D. capensis* in the BUS, the patterns reported here seem to mimic the dispersal patterns of *A. coronus*, from north to south, which are linked to ongoing climate change in the region (Potts et al. 2014; Pringle et al. 2023). Therefore, additional work should be conducted for this species in this system, using genome-wide polymorphisms, to truly discern between these two hypotheses.

Implications for fishery management

Our work identified two diverging *D. capensis* populations across the northern and southern BUS. For conservation and fishery management purposes it is recommended that these two populations be treated as independent evolutionary units owing to the observed complete mitochondrial lineage sorting, reduced ongoing gene flow, as well as the reported biological differentiation between the two populations (Richardson et al. 2011b). Our results also indicate that both populations are likely to have experienced population contractions and expansions, with the southern population contraction being more recent or severe, and the northern population being a potentially older population with higher effective population size and more gene flow. The southern population also shows some evidence of finer-scale sub-structuring which could not be unequivocally identified in this study.

Without fine-scale population structure patterns, it is not possible to locate and protect vulnerable populations within each system and prevent loss of diversity. Adaptive single nucleotide polymorphisms (SNP) potentially can be more effective at assigning individuals to genetic units and investigating evolutionary potentials for fisheries management purposes compared with the limited utility of neutral markers (Schulze et al. 2020). Therefore, further research using putative adaptive loci are required for investigating finer-scale sub-structuring and divergence linked to local adaptation within the northern and southern populations of *D. capensis* to conserve their adaptive capacity and ensure their long-term persistence in a changing ocean.

Acknowledgements — WFO received a National Research Foundation of South Africa MSc support grant (no. 136486). The data were generated under a PhD support grant to RH from Fundação para a Ciência e a Tecnologia, Portugal (ref. SFRH/BD/36176/2007). WMP was supported by funding from the Oppenheimer Generations Research and Conservation program. The authors thank all the commercial, recreational and subsistence fishers that contributed to the sampling effort, especially Paulo Carqueja (Sicopal LDA, Angola), Manuel and Cassiano Henriques (Angola) and Spyker angling tours (Namibia). Perplexity AI was used to assist with text editing.

ORCID

Amber-Robyn Childs: https://orcid.org/0000-0003-4717-2646
Romina Henriques: https://orcid.org/0000-0002-6544-5532
Wilfred Olivier: https://orcid.org/0000-0002-8188-5036
Warren Potts: https://orcid.org/0000-0002-6707-0383
Paul Shaw: https://orcid.org/0000-0003-3594-6798

References

Attwood C, van Zyl CJ, Lombard A, McCagh C. 2016. Seasonally and spatially referenced estimates of recreational shore-angling effort, catch composition, catch rates and total catch in the Goukamma Marine Protected Area, South Africa. *African Journal of Marine Science* 38: 563–579.

Baudouin L, Lebrun P. 2000. An operational Bayesian approach for the identification of sexually reproduced cross-fertilized populations using molecular markers. *International Symposium on Molecular Markers for Characterizing Genotypes and Identifying Cultivars in Horticulture* 546: 81–93.

Bennett RH, Reid K, Gouws G, Bloomer P, Cowley P. 2017. Genetic stock structure of white steenbras *Lithognathus lithognathus* (Cuvier 1829), an overexploited fishery species in South African waters. *African Journal of Marine Science* 39: 27–41.

Berger-Tal O, Saltz D. 2019. Invisible barriers: anthropogenic impacts on inter- and intra-specific interactions as drivers of landscape-independent fragmentation. *Philosophical Transactions of the Royal Society of London, Series B: Biological Sciences* 374: article 20180049.

Bonferroni C. 1936. Teoria statistica delle classi e calcolo delle probabilita. *Pubblicazioni del R Istituto Superiore di Scienze Economiche e Commericiali di Firenze* 8: 3–62.

Buonaccorsi V, McDowell J, Graves J. 2001. Reconciling patterns of inter-ocean molecular variance from four classes of molecular markers in blue marlin (*Makaira nigricans*). *Molecular Ecology* 10: 1179–1196.

Castro JA, Picornell A, Ramon M. 1998. Mitochondrial DNA: a tool for populational genetics studies. *International Microbiology* 1: 327–332.

Chapuis MP, Estoup A. 2007. Microsatellite null alleles and estimation of population differentiation. *Molecular Biology and Evolution* 24: 621–631.

Chessel D, Ollier S, Dray S. 1995. Ordination sous contraintes. *Biométrie et Biologie Évolutive – Université Lyon* 1: 1–69.

Comeros-Raynal MT, Polidoro BA, Broatch J, Mann BQ, Gorman C, Buxton CD et al. 2016. Key predictors of extinction risk in sea breams and porgies (Family: Sparidae). *Biological Conservation* 202: 88–98.

Cornuet JM, Luikart G. 1996. Description and power analysis of two tests for detecting recent population bottlenecks from allele frequency data. *Genetics* 144: 2001–2014.

DFFE (Department of Forestry, Fisheries and the Environment). 2023. *Status of the South African marine fishery resources 2023*. Cape Town, South Africa: DFFE.

Dube K. 2024. A comprehensive review of climatic threats and adaptation of marine biodiversity. *Journal of Marine Science and Engineering* 12: article 344.

Excoffier L, Lischer HE. 2010. Arlequin suite ver 3.5: a new series of programs to perform population genetics analyses under Linux and Windows. *Molecular Ecology Resources* 10: 564–567.

Forde S, von der Heyden S, Le Moan A, Nielsen ES, Durholtz D, Kainge P et al. 2025. Management and conservation implications of cryptic population substructure for two commercially exploited fishes (*Merluccius* spp.) in southern Africa. *Molecular Ecology Resources* 25: e13820.

Fu YX. 1997. Statistical tests of neutrality of mutations against population growth, hitchhiking and background selection. *Genetics* 147: 915–925.

Garnier-Géré P, Chikhi L. 2013. Population subdivision, Hardy–Weinberg equilibrium and the Wahlund effect. In: *eLS 2013 [Encyclopedia of Life Sciences].* New York: Wiley.

Goudet J. 2005. HIERFSTAT, a package for R to compute and test hierarchical *F*-statistics. *Molecular Ecology Notes* 5: 184–186.

Grant WS. 2015. Problems and cautions with sequence mismatch analysis and Bayesian skyline plots to infer historical demography. *Journal of Heredity* 106: 333–346.

Gu Z, Gu L, Eils R, Schlesner M, Brors B. 2014. circlize implements and enhances circular visualization in R. *Bioinformatics (Oxford, England)* 30: 2811–2812.

Gwilliam MP, Winkler AC, Potts WM, Santos CV, Sauer WHH, Shaw PW, McKeown NJ. 2018. Integrated genetic and morphological data support eco-evolutionary divergence of Angolan and South African populations of *Diplodus hottentotus*. *Journal of Fish Biology* 92: 1163–1176.

Hastings RA, Rutterford LA, Freer JJ, Collins RA, Simpson SD, Genner MJ. 2020. Climate change drives poleward increases and equatorward declines in marine species. *Current Biology* 30: 1572–1577.

Healey AJ, Farthing MW, Nunoo FK, Potts WM, Sauer WH, Skujina I et al. 2020. Genetic analysis provides insights into species distribution and population structure in East Atlantic horse mackerel (*Trachurus trachurus* and *T. capensis*). *Journal of Fish Biology* 96: 795–805.

Henriques R, Potts WM, Sauer WHH, Shaw PW. 2012. Evidence of deep genetic divergence between populations of an important recreational fishery species, *Lichia amia* L. 1758, around southern Africa. *African Journal of Marine Science* 34: 585–591.

Henriques R, Potts WM, Sauer WHH, Shaw PW. 2015. Incipient genetic isolation of a temperate migratory coastal sciaenid fish (*Argyrosomus inodorus*) within the Benguela Cold Current system. *Marine Biology Research* 11: 423–429.

Henriques R, Potts WM, Sauer WH, Santos CV, Kruger J, Thomas JA, Shaw PW. 2016a. Molecular genetics, life-history and morphological variation in a coastal warm-temperate sciaenid fish: evidence for an upwelling-driven speciation event. *Journal of Biogeography* 43: 1820–1831.

Henriques R, von der Heyden S, Lipinski MR, du Toit N, Kainge P, Bloomer P, Matthee CA. 2016b. Spatio-temporal genetic structure and the effects of long-term fishing in two partially sympatric offshore demersal fishes. *Molecular Ecology* 25: 5843–5861.

Hoarau G, Boon E, Jongma DN, Ferber SD, Palsson J, van der Veer HW et al. 2005. Low effective population size and evidence for inbreeding in an overexploited flatfish, plaice (*Pleuronectes platessa* L.). *Proceedings of the Royal Society of London, Series B: Biological Sciences* 272: 497–503.

Hutchings L, Lingen Cvd, Shannon LJ, Crawford R, Verheye HM, Bartholomae C et al. 2009. The Benguela Current: an ecosystem of four components. *Progress in Oceanography* 83: 15–32.

Johnson MS, Black R. 1982. Chaotic genetic patchiness in an inter-tidal limpet, *Siphonaria* sp. *Marine Biology* 70: 157–164.

Kapula VK, Ndjaula HON, Schulze M, Durholtz D, Japp D, Singh L et al. 2022. Genetic assessment of seasonal alongshore migration in *Merluccius capensis* in the Benguela region. *Fisheries Research* 250: article 106293.

Kopelman NM, Mayzel J, Jakobsson M, Rosenberg NA, Mayrose I. 2015. Clumpak: a program for identifying clustering modes and packaging population structure inferences across *K*. *Molecular Ecology Resources* 15: 1179–1191.

Leigh JW, Bryant D, Nakagawa S. 2015. POPART: full-feature software for haplotype network construction. *Methods in Ecology and Evolution* 6: 1110–1116.

Lett C, Malauene BS, Hoareau TB, Kaplan DM, Porri F. 2024. Corridors and barriers to marine connectivity around southern Africa. *Marine Ecology Progress Series* 731: 105–127.

Li YL, Liu JX. 2018. StructureSelector: a web-based software to select and visualize the optimal number of clusters using multiple methods. *Molecular Ecology Resources* 18: 176–177.

Luikart G, Allendorf F, Cornuet J, Sherwin W. 1998. Distortion of allele frequency distributions provides a test for recent population bottlenecks. *Journal of Heredity* 89: 238–247.

Lynch M, Ritland K. 1999. Estimation of pairwise relatedness with molecular markers. *Genetics* 152: 1753–1766.

Manel S, Boulanger E, Benestan L, Mouillot D, Dalongeville A. 2023. Revisiting long-distance dispersal in a coastal marine fish. *Ecography* 2023: e06867.

Mann B, Buxton C. 1998. The reproductive biology of *Diplodus sargus capensis* and *D. cervinus hottentotus* (Sparidae) off the south-east Cape coast, South Africa. *Cybium* 22: 31–47.

Mann B, Buxton C, Pollard D, Carpenter K, Sadovy Y. 2009. *Diplodus capensis* W Smith, 1844. *Red List of South African Species*. Pretoria, South Africa: South African National Biodiversity Institute (SANBI). Available at https://speciesstatus.sanbi.org/assessment/last-assessment/2910/ [accessed 27 February 2025].

McKeown N, Hauser L, Shaw P. 2017. Microsatellite genotyping of brown crab *Cancer pagurus* reveals fine-scale selection and 'non-chaotic' genetic patchiness within a high gene-flow system. *Marine Ecology Progress Series* 566: 91–103.

Muller C, Lett C, Porri F, Pattrick P, Bailey D, Denis H et al. DM. 2024. Coastal connectivity of an abundant inshore fish species: model–data comparison along the southern coast of South Africa. *Marine Ecology Progress Series* 731: 89–104.

Nei M. 1987. *Molecular evolutionary genetics*. New York: Columbia University Press.

Nei M, Maruyama T, Chakraborty R. 1975. The bottleneck effect and genetic variability in populations. *Evolution: International Journal of Organic Evolution* 29: 1–10.

Ngeve MN, Van der Stocken T, Menemenlis D, Koedam N, Triest L. 2016. Contrasting effects of historical sea level rise and contemporary ocean currents on regional gene flow of *Rhizophora racemosa* in eastern Atlantic mangroves. *PLoS ONE* 11: e0150950.

O'Reilly PT, Canino MF, Bailey KM, Bentzen P. 2004. Inverse relationship between *F* and microsatellite polymorphism in the marine fish, walleye pollock (*Theragra chalcogramma*): implications for resolving weak population structure. *Molecular Biology* 13: 1799–1814.

Paetkau D. 2004. Direct real-time estimation of migration rate using assignment methods: a simulation-based exploration of accuracy and power. *Molecular* Biology 13: 55–65.

Pascual M, Rives B, Schunter C, Macpherson E. 2017. Impact of life history traits on gene flow: a multispecies systematic review across oceanographic barriers in the Mediterranean Sea. *PLoS ONE* 12: e0176419.

Peakall R, Smouse PE. 2006. GENALEX 6: genetic analysis in Excel. Population genetic software for teaching and research. *Molecular Ecology Notes* 6: 288–295.

Peery MZ, Kirby R, Reid BN, Stoelting R, Doucet-Bëer E, Robinson S et al. 2012. Reliability of genetic bottleneck tests for detecting recent population declines. *Molecular Ecology* 21: 3403–3418.

Pérez L, Infante C, Ponce M, Crespo A, Zuasti E, Funes V et al. 2008. Characterization of eight microsatellite markers in the white sea bream, *Diplodus sargus* (Teleostei, Sparidae). *Molecular Ecology Resources* 8: 1291–1293.

Pew J, Muir PH, Wang J, Frasier TR. 2015. related: an R package for analysing pairwise relatedness from codominant molecular markers. *Molecular Ecology Resources* 15: 557–561.

Piry S, Alapetite A, Cornuet JM, Paetkau D, Baudouin L, Estoup A. 2004. GENECLASS2: a software for genetic assignment and first-generation migrant detection. *Journal of Heredity* 95: 536–539.

Portnoy DS, Puritz JB, Hollenbeck CM, Gelsleichter J, Chapman D, Gold JR. 2015. Selection and sex-biased dispersal in a coastal shark: the influence of philopatry on adaptive variation. *Molecular Ecology* 24: 5877–5885.

Potts WM, Henriques R, Santos CV, Munnik K, Ansorge I, Dufois F et al. 2014. Ocean warming, a rapid distributional shift, and the hybridization of a coastal fish species. *Global Change Biology* 20: 2765–2777.

Pringle BA, Duncan MI, Winkler AC, Mafwila SK, Jagger C, Mckeown NJ et al. 2023. Ocean warming favours a northern *Argyrosomus* species over its southern congener, whereas preliminary metabolic evidence suggests that hybridization may promote their adaptation. *Conservation Physiology* 11: coad026.

Pritchard JK, Stephens M, Donnelly P. 2000. Inference of population structure using multilocus genotype data. *Genetics* 155: 945–959.

Puechmaille SJ. 2016. The program structure does not reliably recover the correct population structure when sampling is uneven: subsampling and new estimators alleviate the problem. *Molecular Ecology Resources* 16: 608–627.

Reid K, Hoareau TB, Graves JE, Potts WM, dos Santos SMR, Klopper AW, Bloomer P. 2016. Secondary contact and asymmetrical gene flow in a cosmopolitan marine fish across the Benguela upwelling zone. *Heredity* 117: 307–315.

Reiss H, Hoarau G, Dickey-Collas M, Wolff WJ. 2009. Genetic population structure of marine fish: mismatch between biological and fisheries management units. *Fish and Fisheries* 10: 361–395.

Richardson TJ, Potts W, Santos C, Sauer WHH. 2011a. Comparison of the population structure and life-history parameters of *Diplodus capensis* (Sparidae) in exploited and unexploited areas of southern Angola. *African Journal of Marine Science* 33: 191–201.

Richardson TJ, Potts WM, Sauer WH. 2011b. The reproductive style of *Diplodus capensis* (Sparidae) in southern Angola: rudimentary hermaphroditism or partial protandry? *African Journal of Marine Science* 33: 321–326.

Roques S, Galarza JA, Macpherson E, Turner GF, Rico C. 2007. Isolation and characterization of nine polymorphic microsatellite markers in the two-banded sea bream (*Diplodus vulgaris*) and cross-species amplification in the white sea bream (*Diplodus sargus*) and the saddled bream (*Oblada melanura*). *Molecular Ecology Notes* 7: 661–663.

Rousset F. 2008. genepop'007: a complete re-implementation of the genepop software for Windows and Linux. *Molecular Ecology Resources* 8: 103–106.

Ryman N, Palm S. 2006. POWSIM: a computer program for assessing statistical power when testing for genetic differentiation. *Molecular Ecology Notes* 6: 600–602.

Sambrook J, Fritsch EF, Maniatis T. 1989. *Molecular cloning: a laboratory manual* (2nd edn). Cold Spring Harbor, New York: Cold Spring Harbor Laboratory Press.

Schulze MJ, von der Heyden S, Japp D, Singh L, Durholtz D, Kapula VK et al. 2020. Supporting fisheries management with genomic tools: a case study of kingklip (*Genypterus capensis*) off southern Africa. *Frontiers in Marine Science* 7: article 557146.

Song YS, Kim JK, Kang JH, Kim SY. 2017. Two new species of the genus *Atractoscion*, and resurrection of the species *Atractoscion atelodus* (Günther 1867) (Perciformes: Sciaenidae). *Zootaxa* 4306: 223–237.

Tajima F. 1989. Statistical method for testing the neutral mutation hypothesis by DNA polymorphism. *Genetics* 123: 585–595.

Tamura K, Nei M. 1993. Estimation of the number of nucleotide substitutions in the control region of mitochondrial DNA in humans and chimpanzees. *Molecular Biology and Evolution* 10: 512–526.

Therkildsen NO. 2012. Insights from the past: retrospective monitoring of genetic variation in Atlantic cod (*Gadus morhua*). PhD thesis, National Institute of Aquatic Resources, Technical University of Denmark, Denmark.

Van Oosterhout C, Hutchinson W, Wills D, Shipley P. 2004. MICRO-CHECKER: software for identifying and correcting genotyping errors in microsatellite data. *Molecular Ecology Notes* 4: 535–538.

Waples RS. 2015. Testing for Hardy–Weinberg proportions: have we lost the plot? *Journal of Heredity* 106: 1–19.

Ward RD, Zemlak TS, Innes BH, Last PR, Hebert PDN. 2005. DNA barcoding Australia's fish species. *Philosophical Transactions of the Royal Society of London, Series B: Biological Sciences* 360: 1847–1857.

Weir BS, Cockerham CC. 1984. Estimating *F*-statistics for the analysis of population structure. *Evolution* 38: 1358–1370.

Wilson GA, Rannala B. 2003. Bayesian inference of recent migration rates using multilocus genotypes. *Genetics* 163: 1177–1191.

Yemane D, Field JG, Griffiths MH. 2004. Effects of fishing on the size and dominance structure of linefish of the Cape region, South Africa. *African Journal of Marine Science* 26: 161–177.

Žužul I, Grubišić L, Šegvić-Bubić T. 2022. Genetic discrimination of wild versus farmed gilthead sea bream *Sparus aurata* using microsatellite markers associated with candidate genes. *Aquatic Living Resources* 35: article 8.

Manuscript received February 2025 / revised August 2025 / accepted August 2025